Acta Metallurgica Sinica (English Letters) (2018) 31:1265–1271
https://doi.org/10.1007/s40195-018-0737-1

A Three-Dimensional Multi-scale Plasticity Model for Metal-Intermetallic Laminate Composites Containing Phases of the $L1_2$ Structure

Yana D. Lipatnikova[1] · Vladimir A. Starenchenko[1] · Yuliya V. Solov'eva[1] · Larisa A. Valuiskaya[2]

Received: 3 January 2018 / Revised: 19 February 2018 / Published online: 25 April 2018

Abstract
A three-dimensional plasticity model was developed and applied to metal-intermetallic laminate composites containing phases of the $L1_2$ structure. A multi-scale approach that combined the methods of continuum mechanics and dislocation kinetics was used. This model takes account of the different mechanisms of self-locking superdislocations, the dislocations and the dislocation walls' density storage for each type of layer at the micro-scale. At the meso-scale, the solutions to the dislocation kinetics equations, in the form of stress–strain curves, were used to create the properties of a three-dimensional representative element. The numerical simulation study of the macroscopic deformation was carried out with the finite element method using the dynamic model of continuum mechanics, which included the classical conservation laws, constitutive equations and the equation of state. It was shown that the simulation results generated using this model were in good agreement with the mechanical tests conducted on the single crystals of the $L1_2$ structure. The model provides an excellent description of the high-temperature plastic strain superlocalization effect of single crystal intermetallics of the $L1_2$ structure. This paper describes the numerical results of the study of the tension and compression tests of metal-intermetallic laminate composites containing phases of the $L1_2$ structure. The model allows the description of the distribution of the accumulated plastic strain inhomogeneities and is capable of predicting the strengthening properties and plastic behaviour of the metal-intermetallic laminate composites containing phases of the $L1_2$ structure.

Keywords Plasticity model · Metal-intermetallic laminate composites · Layered composites, $L1_2$ structure · Tension · Compression

1 Introduction

Laminated metal composite materials currently have great practical applications as structural materials. These materials have excellent mechanical properties: strength, fracture toughness, corrosion and wear resistance, etc. A description of laminates types and the most common methods for obtaining laminates and their properties are presented elsewhere [1]. Metal-intermetallic types of laminated composites also have several advantages: high functional properties, the relative simplicity of production and the low cost. In addition, some have magnetic and electromagnetic shielding properties [2]. Therefore, they are often used in mechanical engineering and are subject to extensive research. These composites are mainly fabricated by bonding the foils of alternating metals. Systems Ti/Al [3–5], Ti/Ni [6–8] and Ni/Al [5, 9] are the most commonly investigated and used. There are many methods of fabrication: hot compaction and hot rolling, explosive welding, reactive sintering, etc. Intermetallic layers, which are formed during the bonding of the foils, have a high strength, hardness and stiffness, whereas more ductile metal layers are intended to make the composite more resistant to brittle fracturing. The topics of experimental research studies have focused on the time and temperature effects on the formation of the phases [4–9], the fracture mechanisms of the intermetallic phase under external

Available online at http://link.springer.com/journal/40195

✉ Yana D. Lipatnikova
yanna_lip@mail.ru

[1] Tomsk State University of Architecture and Building, Solyanaya Sq. 2, Tomsk, Russia 634003

[2] Siberian State Medical University, 2 Moskovsky trakt, Tomsk, Russia 634055

stresses [4–7, 9], the microstructural features of the phases [3], the phases' volume fraction effect on the mechanical properties of the laminates [6–9], etc. However, full-scale experiments do not always make it possible to identify the contributions of the various mechanisms of plastic deformation and to explain the fracture and the development of plastic strain inhomogeneities in a composite material. Therefore, the role of numerical modelling is particularly important for the analysis of the plastic behaviour of the metal-intermetallic layered composite, which allows one to study the loading of composite materials in a wide range of initial conditions within the framework of a unified mathematical approach.

The theoretical research on layered composite materials that is available in the literature is largely based on numerical approaches that were solved within the framework of the finite element method (FEM). A large number of FEM-based studies are devoted to the modelling of fibre-reinforced composites because they have a wide application in the aerospace industry. In a number of studies, the fracture of the deformation of this type of material is carried out within the framework of a micromechanical model using the Generalized Method of Cells [10, 11]. The continuum damage model [12] has been used in other approaches to describe the fracture of the fibre and matrix material. Each of these approaches has its advantages in solving the particular problem. A smaller amount of theoretical work is available in modelling the fracture and deformation of metal-intermetallic layered composite materials, even though they also have great practical applications in the aerospace and engineering industries. The modelling of the deformation and fracture of these composites is usually based on two models [13, 14]: the dynamic model of brittle materials for the intermetallic brittle layer (e.g. in one study [13], the Al_3Ti layer is described by the Johnson-Holmquist ceramics model) and the plasticity model, such as the Johnson–Cook model for a soft metallic layer.

In this paper, in contrast to the approaches noted above, we propose an approach that allows one to take into account the contribution of the accumulation and annihilation of the microdefects of metallic and intermetallic materials. This method makes it possible to describe the deformation hardening of the metal and intermetallic layers whilst taking account of the properties of the microdefects. Our research team has accumulated extensive experience in the experimental and theoretical studies of the plastic behaviour of the intermetallics with the $L1_2$ structure and pure metals with the FCC (face-centred cubic) crystal structure. The structure of $L1_2$ has an FCC cell, in the nodes of which atoms of one type are located, whilst the atoms of another kind are located in the centres of the faces (Fig. 1). Highly detailed studies have been carried out on

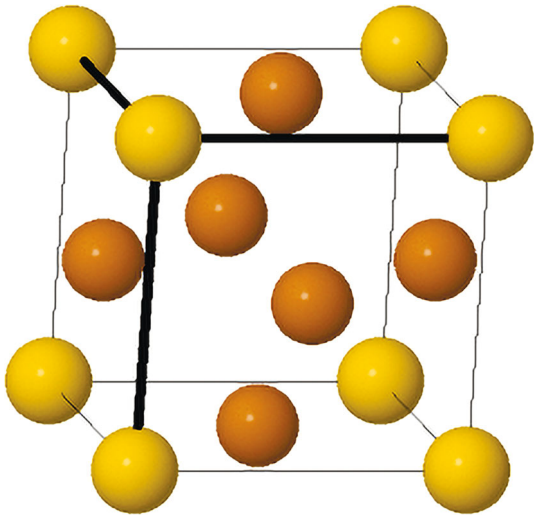

Fig. 1 Unit cell model of the $L1_2$ structure

Ni_3Ge single crystals that are isostructural to Ni_3Al [15–18]. The detailed temperature dependences of the yield and flow stresses have been obtained for the different orientations of single crystals, and the evolution of the dislocation structure of the deformed single crystals has been studied in detail [15, 16]. The use of extensive experimental material has made it possible to obtain the various parameters (the dislocation–dislocation interaction parameter, the effective activation energies of micromechanisms, the value of dislocation density, etc.) necessary to construct the mathematical model of the dislocation kinetics for metals and alloys based on the storage-recovery framework. The constructed mathematical models of the hardening of the medium deformation element for FCC crystal structure pure metals and alloys with the $L1_2$ structure, together with a detailed description of the equation system, are provided in the literature [19–22]. An investigation of the equation system has shown the different types of computational stress–strain curves: periodically or aperiodically damped flow curves, or monotonically increasing hardening curves reaching steady saturation [22]. Thus, in the kinetic model of the mean stress–strain field, various scenarios have been obtained for the development of the deformation of an element of the medium. These scenarios have been confirmed by the experimental observations of the serrated flow of Ni_3Ga, Ni_3Al and Ni3Ge at high temperatures. The originality of the task is the introduction of the obtained scenarios of the element of the deformation medium into the dynamic model of solid mechanics for the description of metal-intermetallic laminate composites. In each layer of the composite, one can set a different scenario for the element of the deformation medium. This will allow us to predict the specific properties and phenomena of the deformation of laminates. It has previously been shown

that simulation results generated using this model were in good agreement with the mechanical tests conducted on the single crystals of the $L1_2$ structure. The model provided an excellent description of the high-temperature plastic strain superlocalization effect of intermetallic single crystals of the $L1_2$ structure [23, 24].

The aim of this study was the development of a three-dimensional plasticity model and its application to metal-intermetallic laminate composites containing phases of the $L1_2$ structure. The calculation tests of the layered rectangular samples of pure metal layers with a volume fraction of 0.3 and the $L1_2$ intermetallic layers with a volume fraction of 0.7 were carried out under uniaxial compression and tension. The laminate layers were perpendicular to the loading axis, and the deformation temperature was set at about 873 K.

2 Three-Dimensional Multi-scale Plasticity Model

2.1 Dislocation Kinetics Model

Dislocation kinetics models of the intermetallic and pure metal phases are based on the storage-recovery framework. A short description of this model is given in this paper. The dislocation kinetics model is described in more detail elsewhere [19].

The equation system includes the balance equation for the dislocation density, the balance equation for the density of the dislocation walls and the equation that describes the shear stresses. The density of the point defects and the coefficients controlling the rearrangement of the dislocations into the dislocation walls do not depend on temperature and stresses. The equation system is as follows:

$$\frac{\mathrm{d}\rho}{\mathrm{d}\varepsilon} = C_1\frac{(\alpha Gb)^2\rho}{\tau}\omega + \frac{C_2\exp(-U_1/\mathrm{kT}) + C_3\exp(-U_2/\mathrm{kT})}{Gb\rho^{1/2}} - \frac{1}{\dot{\varepsilon}}A\frac{\rho^2}{\tau} - \frac{1}{\dot{\varepsilon}}R\rho N + \xi\frac{N}{\Delta h}, \tag{1}$$

$$\frac{\mathrm{d}N}{\mathrm{d}\varepsilon} = I\rho N - \xi N, \tag{2}$$

$$\tau = \tau_f^0 + \gamma_1\tau_0^{(1)}\exp(-U_1/\mathrm{kT}) + \gamma_2\tau_0^{(2)}\exp(-U_2/\mathrm{kT}) + (\alpha_0 - \beta T)Gb\rho^{1/2} + \frac{Gb\mathrm{N}}{4\pi}\mathrm{lg}\left(\frac{1}{Nb}\right), \tag{3}$$

where ρ is the dislocation density; ε is the true strain; $\dot{\varepsilon}$ is the strain rate; C_1, C_2 and C_3 are model coefficients [21]; ω is the fraction of the edge dislocations in the total dislocation density; G is the shear modulus; b is the modulus of the Burgers vector; τ is the shear stress; U_1 and U_2 are the activation energies of the self-locking of the screw and edge dislocations; γ_1 and γ_2 are weight coefficients; $\tau_0^{(1)}$ and $\tau_0^{(2)}$ are pre-exponential factors independent of temperature; N is the density of the dislocation walls; Δh is the average distance between the dislocations in the wall; I, R and ξ are the coefficients controlling the balance of the dislocation walls; A is the annihilation coefficient; α is the parameter of dislocation interaction; and α_0 and β are constants, determined from the experimental dependence $\alpha(T)$ for specific $L1_2$—alloy and pure metal.

The coefficients C_1, C_2 and γ_1, γ_1 are equal to zero in Eqs. (1) and (2) for the pure metal dislocation kinetics model because the terms that contain these coefficients describe the self-locking mechanisms of intermetallics [20, 21].

2.2 Continuum Mechanics Model

It is assumed that the medium is anisotropic and homogeneous within one phase. The mass forces, internal heat sources and thermal effects caused by heat conductivity are absent. On the basis of these assumptions, the continuum mechanics model takes the following form.

$$\frac{\mathrm{d}}{\mathrm{d}t}\int_V \rho\mathrm{d}V = 0, \tag{4}$$

$$\frac{\mathrm{d}}{\mathrm{d}t}\int_V \rho\,\bar{\mathbf{u}}\mathrm{d}V = \int_{\sum} \bar{\mathbf{n}}\cdot\bar{\sigma}\mathrm{d}S, \tag{5}$$

$$\frac{\mathrm{d}}{\mathrm{d}t}\int_V \rho E\mathrm{d}V = \int_{\sum} \bar{\mathbf{n}}\cdot\widehat{\sigma}\cdot\bar{\mathbf{u}}\mathrm{d}S, \tag{6}$$

$$\widehat{\mathbf{e}} = \frac{\overset{\frown}{\mathbf{s}}^{\nabla}}{2\mu} + \lambda\widehat{\mathbf{s}}, \tag{7}$$

$$\widehat{\mathbf{s}} : \widehat{\mathbf{s}} = \frac{2}{3}\sigma_F^2(A_\mathrm{p}), \tag{8}$$

$$p(\upsilon,\ e) = \frac{\rho_0 c_0^2\left(1 - \frac{\in\gamma_0}{2}\right)}{(1 - \zeta\cdot\in)^2} \in +\rho_0\gamma_0 e, \tag{9}$$

where t is time; V is the integration volume; Σ is the surface bounding the volume V; $\vec{\mathbf{n}}$ is the unit vector of the external normal to the surface Σ; ρ is density; $\widehat{\sigma} = -p\widehat{\mathbf{g}} + \widehat{\mathbf{s}}$ is the stress tensor; $\widehat{\mathbf{s}}$ is its deviator; p is pressure; $\widehat{\mathbf{g}}$ is the metric tensor; $\bar{\mathbf{u}}$ is the velocity vector; $E = \varepsilon + \bar{\mathbf{u}}\cdot\bar{\mathbf{u}}/2$ is the specific total energy; e is the specific internal energy;

$$\widehat{\mathbf{e}} = \widehat{\mathbf{d}} - \left(\widehat{\mathbf{d}} : \widehat{\mathbf{g}}\right)\widehat{\mathbf{g}}/3,$$

is the deviator of the deformation rate tensor;

$$\widehat{\mathbf{d}} = \left(\nabla\bar{\mathbf{u}} + \nabla\bar{\mathbf{u}}^T\right)/2,$$

is the deformation rate tensor; $\widehat{\mathbf{s}}^{\nabla}$ is the objective measure of the rate of stress change; μ is the shear modulus; σ_F is the yield stress; A_p is the plastic work of deformation $\in= 1 - V$; c_0 is the volume sound speed in the material; γ_0 is the thermodynamic Grüneisen coefficient; and ζ is the coefficient of linear dependence of the shock wave velocity D on the mass velocity u: $D = c_0 + \zeta u$.

A continuum mechanics model includes mass, momentum and energy conservation laws (4)–(6), constitutive equations of the plastic flow theory (7)–(8) where parameter λ is excluded through the von Mises condition of plasticity (8) and an equation of state (9) in the Mie–Grüneisen form. The flow stress, $\sigma_F = 2\tau$, is used in the form of $\sigma_F = \sigma_{F0}(1 + aA_p + bA_p)$ in Eq. (8), where σ_{F0} is the yield stress ($\varepsilon = 0$) and the coefficients a and b are defined from the strengthening curve that is obtained by the numerical solving of the dislocation kinetics equations system. This enables the strengthening processes of the elementary volume of the deformable object to be taken into account.

The limiting value of the plastic deformation intensity is used as the local criterion of the shear fracture:

$$e_u^* = \frac{\sqrt{2}}{3}\sqrt{3T_2 - T_1^2},$$

where T_1 and T_2 are the first and second invariants of the plastic deformation tensor. The continuum mechanics model has been described in greater detail elsewhere [24, 25].

This model was implemented using the software complex, "RANET-3" [26], with the FEM. This software complex allows for the problems of the dynamic deformation of objects to be solved in a three-dimensional space taking into account the mechanical properties of intermetallic compounds and pure metals.

The medium is continuous in the boundaries between the intermetallic and metal layers. The jump discontinuity of the shear modulus and flow stresses was determined as the boundary condition between layers.

3 Modelling Results

Calculations of the uniaxial tests (compression and tensile) on the rectangular samples of the layered composites at a speed of 30 m/s were carried out. The height of the sample was set at 14 mm, and the ratio of height to length and width was 2:1:1. The width of the layers of pure metal was equal to 1 mm, and for the intermetallic layers, this was 2 mm (Fig. 2).

Figure 3a shows the stress–strain curves obtained through the numerical solving of the set of dislocation kinetics model equations for $L1_2$ alloys (intermetallic-phase stress–strain curve) and pure metals (metal-phase stress–strain curve). These relations set the strain strengthening of the elementary volumes of the appropriate phases. The yield stress of the intermetallics is 800 MPa and the pure metal is 80 MPa. The calculated results of the sample deformation under uniaxial compression are shown in Fig. 3b. The distribution of the intensity of the plastic deformation in the volume of the sample is shown in colour; the true strain is shown by percentage in Fig. 3b. Initial plastic strain is localized in the softer layers of the pure metal (Fig. 3b, at a 12% degree of strain). The elements of the intermetallic phase are involved in the plastic flow process (Fig. 3b at 25% of strain). Further plastic strain is localized in the layers of the pure metal because the strain-hardening coefficient of the intermetallic phase is higher than the metallic one. As a consequence, the sample is fractured, delaminating along soft layers (Fig. 3b at 42% of strain). The laminate stress–strain curve, which was obtained by averaging the von Mises stresses over all elements of the sample, is shown in Fig. 3a. The laminate average stress–strain curve makes an abrupt jump to the yield stress of the intermetallics layers during the initial stage of deformation (0–2% degrees of strain), despite a low yield stress of the metal layers, because the elastic stress of the intermetallic layers is intensively increasing during the deformation of the metal layer. The curve then goes into the strain-hardening stage up to the value of a 33% degree of strain. During this stage, the process of the distribution of the plastic strain occurs both over the elements of the metal and over the elements of the intermetallic compound. The further non-monotonous laminate average stress–strain curve is related to the plastic flow instabilities as a result of the delamination of the composite sample.

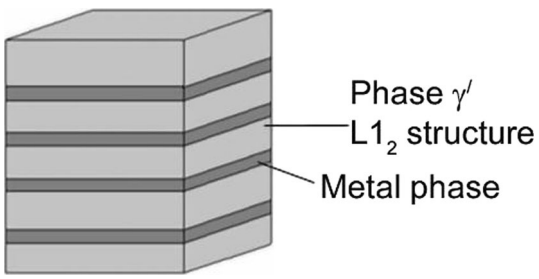

Fig. 2 Model of the layered metal-intermetallic composite

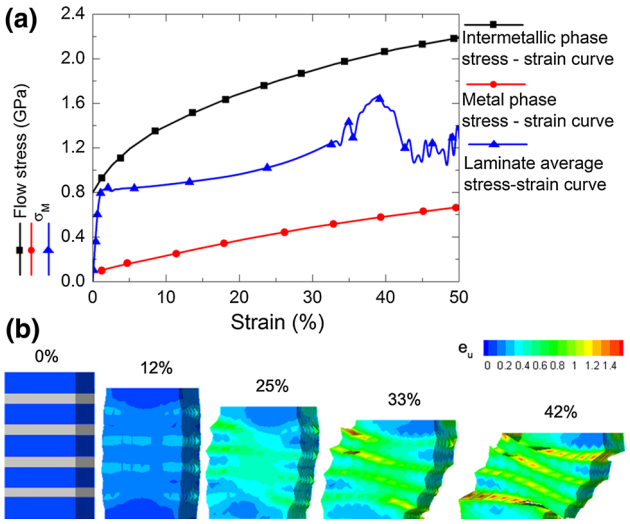

Fig. 3 **a** Stress–strain curves of an elementary volume of each phase and the laminate average stress–strain curve, where σ_M is the von Mises stress, **b** distribution of the plastic strain intensity in the sample under uniaxial compression

A different scenario is observed when the differences between the values of the yield stresses of the different phases are smaller (Fig. 4b). The calculations were made using the higher flow stresses of the metallic phase in comparison with the previous case. The intermetallic-phase stress–strain curve remained unchanged (Fig. 4a). The plastic flow is more homogeneous under these conditions. The blurred deformation localization band is formed (Fig. 4b, 25–34% degree of strain), and its development is then suppressed (Fig. 4b, 50% degree of strain). The laminate average flow stress monotonously increases over the whole range of the considered degrees of strain. This confirms the plastic flow stability, despite the heterogeneous structure of the sample.

The uniaxial tensile tests of the sample were calculated. The curves presented in Fig. 5a show the strengthening of the elementary volumes. The plastic strain intensity patterns are shown in Fig. 5b. The plastic flow begins in the soft metal layers. The elements in the intermetallic layers are included less intensively in the plastic flow than under compression in the same conditions (Fig. 2a). There is a great heterogeneity in the distribution of the plastic strain intensity over the elements of the sample. The fracture of the sample begins at a 36% degree of strain in a few of the metal layers. The laminate average stress–strain curve (Fig. 5a) takes a non-monotonic form throughout the deformation process. A stage of the laminate average stress–strain curve, with a strain-hardening coefficient close to zero (2–20% degrees of strain), follows after the initial stress jump associated with the increase in the elastic stresses in the layers of the intermetallic phase (0–2% degrees of strain). At this time, most of the plastic strain is localized in the metal layers. The flow stress of the laminate average curve then increases (20–29% degrees of strain), and the process of more intensive deformation in the hard intermetallic layers begins. A stage where the strain-hardening coefficient is close to zero (29–36%

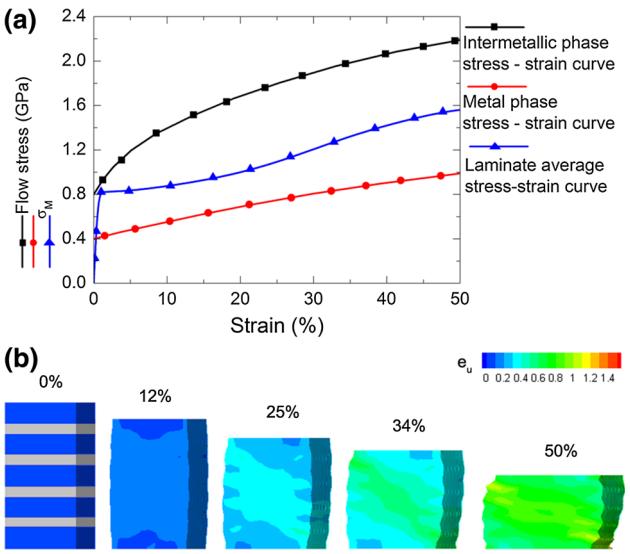

Fig. 4 **a** Stress–strain curves of an elementary volume of each phase and the laminate average stress–strain curve, where σ_M is the von Mises stress, **b** distribution of the plastic strain intensity in the sample under uniaxial compression

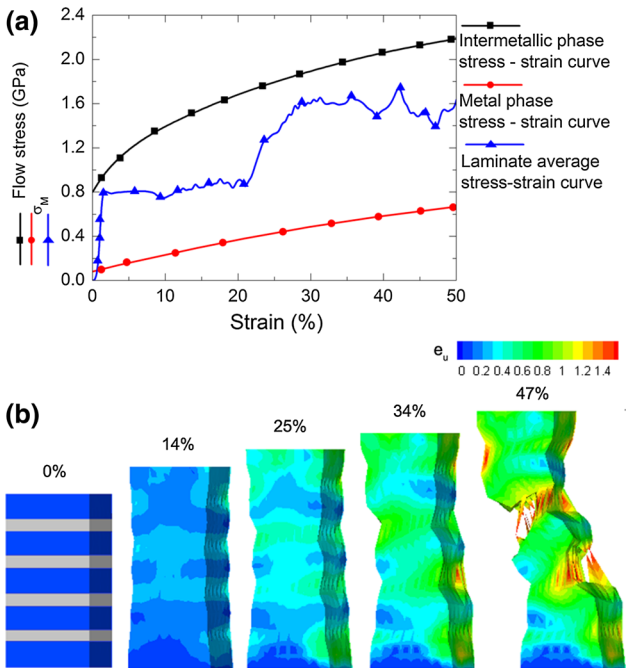

Fig. 5 **a** Stress–strain curves of an elementary volume of each phase and the laminate average stress–strain curve, where σ_M is the von Mises stress, **b** distribution of the plastic strain intensity in the sample under uniaxial tension

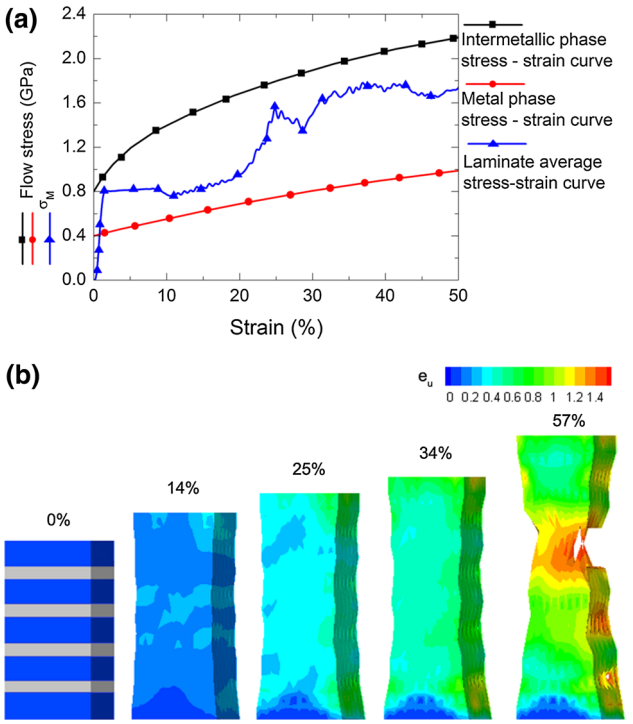

Fig. 6 **a** Stress–strain curves of an elementary volume of each phase and the laminate average stress–strain curve, where σ_M is the von Mises stress, **b** distribution of the plastic strain intensity in the sample under uniaxial tension

degrees of strain) then follows; again, this is due to the plastic strain localization in the soft metal layers. Finally, there are jumps of stresses (36–42% degrees of strain) associated with the beginnings of the laminate sample failures.

A more homogeneous distribution of plastic strain intensity along the laminate sample is observed in calculations with a higher yield stress in the metal phase than in the previous case. A later process of failure is observed (at a 55% degree of strain) as a consequence. The laminate average stress–strain curve (Fig. 6a) takes a similar form to the curve in the previous case (Fig. 5a) but there are also differences: the stage with a low hardening coefficient (2–9%) is less extended and the strain-hardening process begins earlier and is associated with a more intensive distribution of plastic strain along the intermetallic layers.

4 Conclusions

The effect of the strength of pure metal layers on the plastic behaviour of laminate composite has been analysed using a three-dimensional multi-scale plasticity model for metal-intermetallic laminate composites containing phases of the $L1_2$ structure.

1. The change of the yield stress of the pure metal layers has little effect on the calculations of the laminate average stress–strain curve for both tensile and compression. The calculated laminate average stress–strain curve changed by less than 10% after a fivefold increase in the yield stress of the pure metal layers.
2. The strength of the metal layers significantly affects the homogeneity and stability of the plastic flow of the laminate. The lower the yield stress of the metal layer, the more heterogeneous is the distribution of the plastic strain intensity across the sample. An earlier fracture of the laminate was observed, and this is associated with delamination during compression and failure under tension at places in the soft metal layers.
3. The calculations show non-monotonous tensile laminate average stress–strain curves that can be explained by the strain localization in the soft metal layers.
4. The shape of the laminate average stress–strain curve differs significantly from the shape of the stress–strain curves of the metal and intermetallic layers. New strain-hardening stages emerged that were associated with the influence of the heterogeneous-layered structure of the material.
5. More homogeneous distribution of the plastic strain intensity over the sample was observed under compression. In percentage terms, the stress–strain curves are strictly monotonic up to 30 degrees of strain.

Acknowledgement The work was financially supported by the Russian Science Foundation (No. 17-72-10042).

References

[1] D.R. Lesuer, C.K. Syn, O.D. Sherby, J. Wadsworth, J.J. Lewandowski, W.H. Hunt, J. Int. Mater. Rev. **41**, 169 (1996)
[2] X. Ma, Q. Zhang, X. Chen, G. Wu, Acta Metall. Sin. (Engl. Lett.) **27**, 918 (2014)
[3] Y. Du, G. Fan, T. Yu, N. Hansen, L. Geng, X. Huang, Effects of interface roughness on the annealing behaviour of laminated Ti-Al composite deformed by hot rolling. in *IOP Conference Series: Materials Science and Engineering*. vol. 89 (2015)
[4] L. Qin, J. Wang, Q. Wu, X. Guo, J. Tao, J. Alloys Compd. **712**, 69 (2017)
[5] D.E. Alman, C.P. Dogan, J.A. Hawk, J.C. Rawers, Mater. Sci. Eng. A **192**, 624 (1995)
[6] Y. Zhang, X. Cheng, H. Cai, Mater. Des. **92**, 486 (2016)
[7] Y. Zhang, X. Cheng, H. Cai, H. Zhang, J. Alloys Compd. **699**, 695 (2017)
[8] A. Patselov, B. Greenberg, S. Gladkovskii, R. Lavrikov, E. Borodin, AASRI Proced. **3**, 107 (2012)
[9] Y. Guo, Z. Shi, Y. Xu, G. Qiao, J. Wang, Rare Metal Mater. Eng. **43**, 813 (2014)
[10] D. Ivančević, I. Smojver, Compos. Struct. **145**, 248 (2016)
[11] D. Ivančević, I. Smojver, Compos. Struct. **145**, 259 (2016)
[12] N. Zobeiry, A. Forghani, C. McGregor, S. McClennan, R. Vaziri, A. Poursartip, Compos. Struct. **173**, 188 (2017)

[13] T. Li, F. Grignon, D.J. Benson, K.S. Vecchio, E.A. Olevsky, F. Jiang, A. Rohatgi, R.B. Schwarz, M.A. Meyers, Mater. Sci. Eng. A **374**, 10 (2004)
[14] Y. Cao, C. Guo, S. Zhu, N. Wei, R.A. Javed, F. Jiang, Mater. Sci. Eng. A **637**, 235 (2015)
[15] V.A. Starenchenko, E.V. Kozlov, Y.V. Solov'eva, Y.A. Abzaev, N.A. Koneva, Mater. Sci. Eng. A **483–484**, 602 (2008)
[16] N.A. Koneva, Y.V. Solov'eva, V.A. Starenchenko, E.V. Kozlov, Mater. Res. Soc. Symp. P **842**, S5.25.1–S5.25.6 (2004)
[17] V.A. Starenchenko, Y.V. Solov'eva, S.V. Starenchenko, Bull. Rus. Acad. Sci. Phys. **77**, 1091 (2013)
[18] Y.V. Solov'eva, E.L. Nikonenko, S.V. Starenchenko, V.A. Starenchenko, Bull. Rus. Acad. Sci. Phys. **75**, 673 (2011)
[19] V.A. Starenchenko, Y.V. Solov'eva, Y.A. Abzaev, Phys. Solid State **41**, 407 (1999)
[20] V.A. Starenchenko, D.N. Cherepanov, Y.V. Solov'eva, L.E. Popov, Rus. Phys. J. **52**, 398 (2009)
[21] V.A. Starenchenko, D.N. Cherepanov, O.V. Selivanikova, Rus. Phys. J. **57**, 139 (2014)
[22] V.A. Starenchenko, Y.V. Solov'eva, Y.D. Fakhrutdinova, L.A. Valuiskaya, Rus. Phys. J. **54**, 885 (2012)
[23] V.A. Starenchenko, L.A. Valuiskaya, Y.D. Fakhrutdinova, Y.V. Solovjeva, N.N. Belov, Rus. Phys. J. **55**, 211 (2012)
[24] Y.V. Solov'eva, Y.D. Fakhrutdinova, V.A. Starenchenko, Phys. Met. Metalogr. **116**, 10 (2015)
[25] N.N. Belov, D.G. Kopanitsa, N.T. Yugov, *Mathematical Simulation of Dynamic Strength of Constructional Materials* (STT, Tomsk, 2010)
[26] N.T. Yugov, N.N. Belov, A.A. Yugov, Calculation of adiabatic nonstationary flows in the three-dimensional formulation (RANET-3), Russian Federation Patent No. 2010611042, (2010)